Proceedings of the 35th European Safety and Reliability & the 33rd Society for Risk Analysis Europe Conference
Edited by Eirik Bjorheim Abrahamsen, Terje Aven, Frederic Bouder, Roger Flage, Marja Ylönen
 Published by Research Publishing, Singapore.
doi: 10.3850/978-981-94-3281-3_ESREL-SRA-E2025-P7883-cd

An Improved Subset Sampling Method and Application in High Cycle Fatigue Reliability Assessment of a Mistuned Composite Fan Bladed Disk Assembly

Xu Tang

School of Mechanical Engineering, Shanghai Jiao Tong University, China. E-mail: t1996422@situ.edu.cn

Yong Chen

School of Mechanical Engineering, Shanghai Jiao Tong University, China. E-mail: yongchen@situ.edu.cn

Carbon fiber reinforced plastics (CFRP) are characterized by the outstanding mechanical properties. Many corporations are developing this kind of composite fan blades and apply to the next generation high-bypass-ratio turbofan engines. Stochastic sources always cause discrepancy between realizations and nominal design, e.g. raw material strength, manufacturing tolerance, defect and damage (crack), assembly, service environment, etc. The current focus of probabilistic safety design for gas turbine components have been put on efficiently evaluating the reliability index.

The objective of this study is to derive an efficient approach to evaluate the risk of a structural mistuned fan stage subject to vibration-induced high cycle fatigue (HCF). The stochastic variable is failure probability of a single composite fan blade based on corresponding probabilistic design curve in one of typical vibration modes. Since crude Monte Carlo simulation (MCS) is strongly dependent on probability of rare event, subset simulation (SS) is a remedy for this limitation by separating failure domain into a series of intermediate regions. The target probability is a product of auxiliary conditional failure probability with intermediate thresholds. However, low acceptance rate via the classical Metropolis-Hastings Markov chain Monte Carlo (MCMC) simulation leads to erroneous estimates of conditional probability. In the proposed ensemble subset sampler (ESS), Markov chain is generated by affine invariant ensemble algorithm that the acceptance rate of candidate points is increased by generating proposal samples using stretch move. Through conducting simple validation cases to compare performance with SS, the proposed method would reduce the number of limit state function evaluations and increase numerical accuracy. It is then fully integrated into composite fan blade-disk finite element (FE) model. Intermediate conditional failure probabilities are calculated with the distributed surrogate models for steady and vibratory stresses. The application further demonstrates good performance to a typical mistuning pattern for fan-disk assembly.
Keywords: subset sampling, ensemble sampler, structural mistuning, high cycle fatigue, composite fan blades.

1. Introduction

CFRP is characterized by the outstanding mechanical properties. Many aero engine corporations are developing the preferred fan blades consisting of unidirectional CFRP prepregs and apply to the next generation high-bypass-ratio turbofan engines [1]. Stochastic sources cause discrepancies between realizations and the nominal design, e.g. raw material strengths, manufacturing tolerances, defects and damages (cracks), assembly, service environment, etc. The current focus of probabilistic safety design for gas turbine rotor components have been put on efficiently evaluating the reliability index. It could give an accurate evaluation for the potential risk of failure when all these uncertainties are incorporated, whereas an empirical safety factor determined the design allowable, but not able to give the safety level. The component is deemed to be safe even if applied stress is larger than the design allowable. The MCS is the most convenient methodology to assess the failure probability only if the joint probability density of input random vector is known and a closed-form forward prediction model is available. However, numerical simulation, e.g. finite element procedure, is time-consuming to obtain the target response mandatory in structural design criteria, e.g. HCF failure due to forced vibrations. Hence, it is impossible to evaluate the reliability

especially for rotor blades conforming to rigorous airworthiness requirements. An ease-of-use and efficient sampler is attractive for structural reliability analysis of composite fan blades.

There is currently three categories of method, i.e. local series expansion, direct simulations, metamodels, to evaluate structural failure probability. For all these methods, a limit state function should be formulated to indicate the failure domain and its boundaries. However, both metamodel-based and series expansion are especially widely used in engineering field but imposed extra approximation errors on the numerical models which always exists in practice. Thus, the simulation method has the most accurate predictions if difficulty in computational cost could be resolved. Among them, SS, firstly proposed by Au and Beck [2], is an efficient method in most application case since the target limit state function is divided into a series of sub-domains which can be easily solved by Metropolis algorithm. Lang et al. [3] had compared several Markov chain Monte Carlo (MCMC) algorithms used in SS, he found that the preconditioned Crank-Nicolson and conditional sampling algorithms had the higher performance in relative errors and variabilities of failure probability. Goodman et al. [4] proposed an affine invariant ensemble sampling technique to deal with a poorly-scaled and highly-anisotropic target distributions, where the classical Metropolis Hastings algorithm must be modified to be efficient in simulation. If there is an affine transformation of original target posterior distribution, the simulation extracts samples from an easier posterior distribution. Lye and Reiner [5-6] both applied the affine invariant ensemble sampler (AIES) in Bayesian inference for uncertainty in progressive damage simulation of composites as well as coupled oscillator system. Xiao et al. [7] has extended the SS to formulate a two-stage MCMC simulation in evaluating the reliability sensitivity analysis which is usually hard to calculate for rare event. To the best of author knowledge, the SS currently shows its potentials in reliability analysis with relevance to engineering design.

This study is mainly tried to assess the reliability of composite fan blade-disk system due to forced excitations using the modified subset simulation. The proposal samples in each iteration of MCMC simulation is given by ESS to obtain the steady Markov chains with a higher acceptance rate. Thus, it provide an accurate estimate of intermediate failure domains. The proposed method is compared with the classical SS when applied to evaluate some simple rare event reliability problems, which shows an improved efficiency. Then, the associated limit state function is defined based on the weakest-link theory to describe HCF failure probability, ESS shows an improved prediction accuracy in failure probability prediction for mistuned fan-disk assembly.

2. Simulation Method

For a structural reliability analysis, the limit state function $g(\boldsymbol{x})$ in sample space D is written as Eq.(1), where $\boldsymbol{x}$ denotes input random vector with dimension d, and $I(\cdot)$ is the indicator function.

$$P_{\mathrm{f}} = \int_{x\in D} I(g(\boldsymbol{x}))\pi(\boldsymbol{x})\mathrm{d}\boldsymbol{x} \tag{1}$$

2.1. *Subset simulation*

In a conventional subset simulation algorithm for rare event probability estimation, the total failure domain D_{f} is separated into a series of subdomains, which satisfies $D=D_0\supset D_1\supset D_2\cdots\supset D_k=D_{\mathrm{f}}$. The intermediate failure domain is defined by $g(\boldsymbol{x})\leqslant t_k$ $(k=1,\cdots,m)$, i.e. $D_k=\{\boldsymbol{x}:g(\boldsymbol{x})\leqslant t_k\}$, where t_k is intermediate failure threshold. Thereafter, the original probability mass could be formulated as Eq.(2). The intermediate probability density function (PDF) $\pi_k(\boldsymbol{x})$ is given in Eq.(3), the optimum sampling distribution in importance sampling.

$$P_{\mathrm{f}} = P(\cap_{k=0}^{m} D_k) = P(D_0)\prod_{k=1}^{m} P(D_k \,|\, D_{k-1}) \tag{2}$$

$$\pi_{D_{k-1}}(\boldsymbol{x}) = \begin{cases} \dfrac{I(g(\boldsymbol{x})\leq t_{k-1})\pi(\boldsymbol{x})}{P(\mathcal{D}_{k-1})} & \boldsymbol{x}\in\mathcal{D}_{k-1} \\ 0 & \boldsymbol{x}\notin\mathcal{D}_{k-1} \end{cases} \tag{3}$$

To obtain the samples conforming to the these PDFs, MCMC simulation is used to draw samples. t_k is determined by order statistic, then Eq.(2) is re-arranged as $P_{\mathrm{f}} = P_0^m P_m$, where P_0 is the conditional probability at the empirical quantile computed by MCS samples, and $P_m = \Sigma I(g(\boldsymbol{x})\leq t_k)/N_k$, denotes the failure probability in

the last subdomain D_k where the intermediate failure threshold t_k equals to 0. Based on the modified MCMC simulation introduced by Au and Beck, evaluation of coefficient of variation (CV) for P_f estimate is given in Eq.(4), where P_0 is fixed to achieve an balance between number of subdomain and accuracy of quantile estimation, $\rho_k(n)$ is the average n-lag auto-correlation coefficient in the kth subset, with the total number of N_k=CN samples in the kth level. Hence SS has a maximum of N_T=mN_k times to call limit state function.

$$\begin{aligned} \mathrm{CV}(P_f) &= \sqrt{\sum_{k=1}^{m}\delta_k^2} \\ \delta_k &= \sqrt{\frac{1-P_k}{N_k P_k}\left(1+2\sum_{n=1}^{N-1}\left(1-\frac{n}{N}\right)\rho_k(n)\right)} \end{aligned} \tag{4}$$

$$\rho_k(n) = \frac{\mathrm{Corr}(I(g(\boldsymbol{x}_j)\le t_k), I(g(\boldsymbol{x}_{j+n})\le t_k))}{\mathrm{Corr}(I(g(\boldsymbol{x}_j)\le t_k), I(g(\boldsymbol{x}_j)\le t_k))} \tag{5}$$

When the intermediate probability $\pi_k(\boldsymbol{x})$ is seen as the posterior distribution in Bayes′ theorem, it is an update of an underlying prior distribution. The Markov chain is convergent to the target distribution using MCMC simulation if the detailed balance condition given in Eq.(6) is upheld for all iteration n. Metropolis Hastings algorithm draws samples in Eq.(7) from a multivariate Gaussian proposal PDF $p(\cdot)$, where a is a scale factor for prior covariance matrix. In addition, the proposal distribution is not exactly the state transition probability $k(\cdot)$ between adjacent steps in a Markov chain, thus the second term in Eq.(8) does not equal to 1. The resulting state transition probability is given in Eq.(9). A sample $u \in [0,1]$ is drawn from the standard uniform distribution to improve the convergence rate and avoid burn-in. The candidate sample is rejected, i.e. $\boldsymbol{x}^{n+1} = \boldsymbol{x}^n$, when $\alpha(\boldsymbol{x}^n, \boldsymbol{x}^*) < u$.

$$\pi(\boldsymbol{x}^n)k(\boldsymbol{x}^{n+1}\,|\,\boldsymbol{x}^n) = \pi(\boldsymbol{x}^{n+1})k(\boldsymbol{x}^n\,|\,\boldsymbol{x}^{n+1}) \tag{6}$$

$$\boldsymbol{x}^* = \boldsymbol{x}^n + \boldsymbol{x}^p, \quad \boldsymbol{x}^p \sim N(0, a\boldsymbol{I}) \tag{7}$$

$$\alpha(\boldsymbol{x}^*, \boldsymbol{x}^n) = \min\left(1, \frac{\pi(\boldsymbol{x}^*)p(\boldsymbol{x}^n\,|\,\boldsymbol{x}^*)}{\pi(\boldsymbol{x}^n)p(\boldsymbol{x}^*\,|\,\boldsymbol{x}^n)}\right) \tag{8}$$

$$k(\boldsymbol{x}^*\,|\,\boldsymbol{x}^n) = p(\boldsymbol{x}^*\,|\,\boldsymbol{x}^n)\alpha(\boldsymbol{x}^*, \boldsymbol{x}^n), \ \forall \boldsymbol{x}^* \tag{9}$$

Proposal distribution $p(\boldsymbol{x}^*|\boldsymbol{x}^j)$ should be as similar to the posterior distribution as possible since a badly chosen proposal distribution significantly affects the MCMC performance so that proposed samples are nearly all rejected based on Eq.(8). Therefore, samples in subset D_k is not convergent to target distribution under a limited number of iterations, which weakens the efficiency of subset sampling algorithm and resulting estimate accuracy of t_m. In the worst case, it is fully degraded into the crude MCS when there is little overlapping area between two PDFs.

2.2. *Ensemble subset sampler*

AIES runs a set of C Markov chains, the chain locations $\boldsymbol{x}_c$ (c=1,⋯,C) are updated by an set of chains in previous iteration. The affine invariance property is achieved by generating proposals according to strength move showed in Eq.(10), where $\tilde{n} = n+1$ if $i < c$ and $\tilde{n} = n$ when $i \geqslant c$. To ensure the generalized proposal distribution is symmetrical, PDF of random variable z should satisfy the equation, i.e. $\pi_z(z)$= $z\pi_z(1/z)$. One of PDFs in this cluster is given in Eq.(11), where a denotes a scalar turning parameter as that in MH sampler. The proposal candidate is then accepted as new location of the cth chain with probability in Eq.(12).

$$\boldsymbol{x}_c^* = \boldsymbol{x}_i^{\tilde{n}} + z\cdot\left(\boldsymbol{x}_c^n - \boldsymbol{x}_i^{\tilde{n}}\right) \tag{10}$$

$$\pi(z\,|\,a) = \begin{cases} \dfrac{1}{\sqrt{z}(2\sqrt{a} - \dfrac{2}{\sqrt{a}})} & \dfrac{1}{a} \le z \le a \\ 0 & \text{otherwise} \end{cases} \tag{11}$$

$$\alpha\left(\boldsymbol{x}_c^*, \boldsymbol{x}_c^n, z\right) = \min\left\{1, z^{d-1}\frac{\pi(\boldsymbol{x}_c^*)}{\pi(\boldsymbol{x}_c^n)}\right\} \tag{12}$$

The N_s samplers constitute an ensemble subset sampler, called ESS, which fully leverages advantages of each sampler. In this study, the ensemble contains two samplers as introduced above. Since each sampler predicts a respective failure probability denoted as P_f^l (l=1,⋯,N_s), ESS gives a weighted failure probability estimation in Eq.(13). The weight coefficient depends on the computation cost Δt_l for which sampler implements a SS, where a more efficient sampler has a larger weight.

$$P_f = \sum_{l=1}^{N_s}\left(1 - \frac{\Delta t_l}{\sum_{l=1}^{2}\Delta t_l}\right)P_f^l \tag{13}$$

2.3. *Sampler integration*

Many studies [5,7] have reported an optimal acceptance rate is 0.44 for failure probability estimation. An adaptive acceptance rate scheme is given in Eq.(14), where parameter a_k^j is adjusted in each iteration batch j to be the target acceptance rate $r^*=0.21d^{-0.5}+0.23$. When the acceptance rate r_k^j of N_s samples is less than the target value, a smaller a_k^{j+1} is used in the next iteration and vice versa.

$$a_k^{j+1} = a_k^j \exp\left(\frac{r_k^j - r^*}{j}\right) \tag{14}$$

The Gelman-Rubin diagnostic r_{GB} [8] acts as an indicator to terminate sampler. It is calculated by two covariance matrices defined in Eqs.(15-16). The basic motivation is intuitive: the average covariance matrix $\boldsymbol{W}$ between C individual Markov chains should be same as covariance matrix $\boldsymbol{B}$ between C individual average statistics $\bar{\boldsymbol{x}}_c$, where $\boldsymbol{WB}$ equals to $\boldsymbol{BW}$. The maximum eigenvalue $\lambda_{\max}$ of matrix $\boldsymbol{W}^{-1}\boldsymbol{B}$ is used to compute r_k^{GB} in Eq.(17).

$$\boldsymbol{W} = \frac{\sum_{c=1}^{C}\sum_{n=1}^{N}(\boldsymbol{x}_c^n - \bar{\boldsymbol{x}}_c)(\boldsymbol{x}_c^n - \bar{\boldsymbol{x}}_c)^{\mathrm{T}}}{C(N-1)} \tag{15}$$

$$\bar{\boldsymbol{x}}_c = \frac{1}{N}\sum_{n=1}^{N}\boldsymbol{x}_c^n$$

$$\boldsymbol{B} = \frac{\sum_{c=1}^{C}(\bar{\boldsymbol{x}}_c - \bar{\bar{\boldsymbol{x}}})(\bar{\boldsymbol{x}}_c - \bar{\bar{\boldsymbol{x}}})^{\mathrm{T}}}{C-1} \tag{16}$$

$$\bar{\bar{\boldsymbol{x}}} = \frac{1}{NC}\sum_{c=1}^{C}\sum_{n=1}^{N}\boldsymbol{x}_c^n$$

$$r_k^{\mathrm{GB}} = \frac{N\text{-}1}{N} + \frac{C+1}{C}\lambda_{\max} \tag{17}$$

The procedure of ESS is listed in Fig.1. It is capable of evaluating the failure probability of rare event without increasing times of limit state function call. A small proportion of failed samples in the last subdomain is transferred into the Markov chain as the initial samples, which guarantees the acceptance criterion is not divided by zero. Therefore, the numerical instabilities is avoided when the proposal sample always lies in the failure domain of these sub reliability analyses.

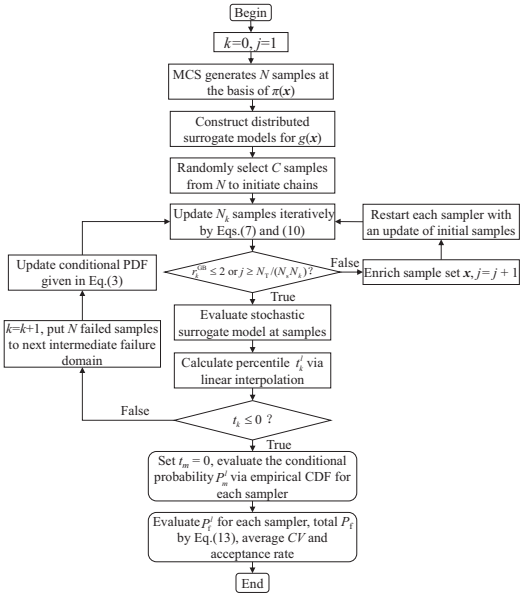

Fig. 1. Procedure of the proposed ESS.

3. Test Cases

In this section, the proposed ESS algorithm is firstly validated against two simple test cases. Among them, the limit state functions are in analytical forms with much smaller time costs than the FE models in engineering application. It should be noted that the MCS provide a reference failure probability for both ESS and SS.

3.1. *2D function*

The first analytical example is a two-dimensional limit state function presented in [7], which is given in Eq.(18). There is only one failure region boundary, representing a category of limit state function, e.g. parallel system. The joint probability function of input variables conforms to a two dimensional Gaussian distribution. The failure probability is calculated as 3.35×10^{-4} in total 5×10^7 samples by using the MCS. In addition, the N_k, C, and P_0 in SS are set 10000, 10 and 0.1, with a maximum of 5 adaptive update steps.

$$g(\boldsymbol{x}) = 2.5 - x_2 + \exp(-x_1^2/10) + (x_1/5)^4 \tag{18}$$

Their comparisons between computation time, *CV*s and acceptance rate is listed in Table 1. Both methods applies significantly less limit function calls than MCS. The ESS provides a relative estimation error 34.32%, a bit smaller than 41.49% by SS at same number of samples. Moreover, computation time decrease by 57.93%, showing advantage in efficiency over MCS. In Table 2, SS has an inferior prediction accuracy than ESS due to much larger acceptance rate which demonstrates SS does not fully explore the failure domain. It should be noted that, when limit state function is analytical, MCS needs only more than a few seconds, but for time-consuming models, the increasing time is more obvious.

Table 1. Performance comparisons in case 1.

Method	P_f	Time / s	CV / %	r
MCS	3.35×10^{-4}	4.16	0.77	1.00
SS	1.96×10^{-4}	0.10	13.34	0.91
ESS	4.50×10^{-4}	1.75	29.72	0.41

Table 2. The intermediate failure thresholds in case 1.

Method	t_1	t_2	t_3	t_4
SS	2.12	1.05	0.36	0.00
ESS	2.14	1.22	0.62	0.00

3.2. *Tantem system*

The second example concentrates on a tandem system with higher reliability. A two-dimensional limit state function is defined in Eq.(19), which is an union of individual limit state function $g_e(\boldsymbol{x})$ (e=1,⋯,4). Input variables are Gaussian and mutually independent. In addition to a lower P_f , the failure domain contains four disconnected regions, filling with alternate safety regions. It poses a relatively large challenge to sampler although the initial MCS samples are populated within the whole random space. When initial samples are not all lied at these regions, part of Markov chains would have a low acceptance rate, therefore higher autocorrelation coefficient in this level of subset sampling. Moreover, the high correlated samples is used as the initial seeds of multiple chains, further affecting conditional failure probability estimate at the next level. The accumulated errors eventually are expected to result in a smaller P_f. In perspective of structural design, the biased total failure probability provides conservative but undesired prediction for aeroengine component reliability in comparison with adopting an empirical knock-down safety factor.

$$g(\boldsymbol{x}) = \bigcup_{e=1}^{4}\{g_e \le 0\} = \min\left\{\begin{array}{c} 0.1(x_1-x_2)^2 - \dfrac{(x_1+x_2)}{\sqrt{2}} + \dfrac{9}{2} \\ 0.1(x_1-x_2)^2 + \dfrac{(x_1+x_2)}{\sqrt{2}} + \dfrac{9}{2} \\ x_1 - x_2 + \dfrac{9\sqrt{2}}{2} \\ x_2 - x_1 + \dfrac{9\sqrt{2}}{2} \end{array}\right\} \tag{19}$$

MCS provides a P_f estimate of 1.42×10^{-5} with CV less than 5% in total 5×10^7 samples. Parameters in subset sampling is same as the first case. In Table 3, SS predicts failure probability deviating from reference value by -65.70%, over which ESS has an overwhelming advantage. As mentioned before, SS sampler does not fully explore target distribution and introduces dependence between successive samples, whereas ESS quickly obtains intermediate failure thresholds closer to failure boundary. Except for the high correlation between samples from a Markov chain, ESS consumes too much time at each conditional level to ensure r^{GB} less than 2. However, the slightly increased cost does not hide the truth that ESS is able to predict failure probability with an optimum acceptance rate. Simulation process is showed in Fig.2, it intuitively showcases failure boundary as well as how ESS obtain failure samples within six nested levels.

Table 3. Performance comparisons in case 2.

Sampler	P_f	Time / s	CV / %	r
MCS	1.14×10^{-5}	4.62	4.18	1.00
SS	3.91×10^{-6}	0.10	16.23	0.86
ESS	6.57×10^{-6}	10.82	32.57	0.41

Table 4. The intermediate failure thresholds in case 2.

Sampler	t_1	t_2	t_3	t_4	t_5	t_6
SS	2.91	2.01	1.24	0.65	0.19	0.00
ESS	2.93	1.80	1.11	0.59	0.11	0.00

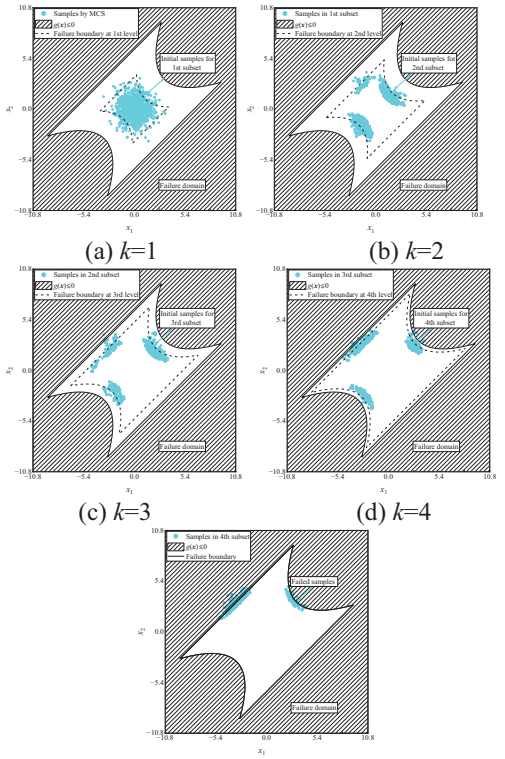

(a) k=1 (b) k=2

(c) k=3 (d) k=4

(e) k=5

Fig. 2. Samples of tandem system during ESS evaluation process.

The parallel sampling scheme also does not guarantee each region has at least one sample given at finite sample size especially when density of disconnected regions increases. For moderate complex tandem system in engineering application, however, it is reasonable to suppose that size of these regions is less than N_k, giving rise to a negligible performance degradation.

4. Engineering Application

The FE composite fan blade model runs with a batch mode, where layup design for composite material and applied boundary conditions are disclosed in [9]. It is supposed that only the longitudinal engineering elastic modulus is the only the uncertainty source which could be represented using the continuous PDF type. Variability of elastic modulus results in the vibration characteristics, i.e. natural frequencies and mode shapes, and the harmonic responses under aerodynamic force excitations. The structural mistuning is simplified to be known and formulated in Eq.(20), where $\Delta \boldsymbol{E}_1=[\Delta E_1^1, \cdots, \Delta E_1^s, \cdots \Delta E_1^{N_b}]$ follows the pattern in Fig.3. The first component of random vector $\boldsymbol{x}$ is a standard Gaussian marginal, i.e. $x_1 \sim N(0,1)$, and CV=10%. Excitation frequencies is fixed whatever natural frequencies of mistuned fan-blade assembly varies to.

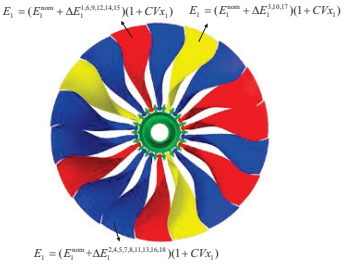

(a) Typical mistuning pattern

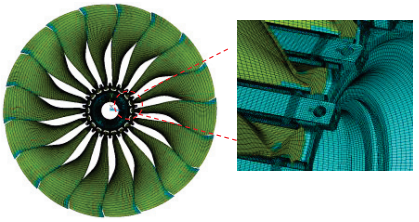

(b) Finite element model

Fig. 3. Physical model of mistuned composite fan blade-disk system.

$$\boldsymbol{E}_1=(\boldsymbol{E}_{1,\mathrm{nom}}+\Delta \boldsymbol{E}_1)(1+CVx_1) \tag{20}$$

In this case, a stochastic surrogate model is constructed to replace structural stress responses $\sigma_{\mathrm{s/a}}$ of the sth sector at the basis of non-intrusive polynomial expansion (PCE) in Eq.(21)

$$\sigma_{\mathrm{s/a}} \approx M(x_1)=\sum_p y_p^s \psi_p^s(x_1) \tag{21}$$

The univariate Hermite polynomials actually corresponds to a series of orthonormal base functions in original domain D_0. In this scenario, the pth degree polynomial base ψ_k^p ($k\neq 0$) is constructed by reference to [10]. These coefficients are calculated using ordinary least square regression.

When material fatigue limit is less than the applied vibratory stress, composite fan blade is failed and the underlying design parameter set

located at failure domain. Moreover, the fatigue limit of carbon fiber reinforced composite material follows a Weibull distribution when it is subject to a uniform load based on the Weakest-link theory [11-12], which supposes the microcracks uniformly locate in the structural volume consisting of brittle material. For the fan blade-disk assembly system, considering failure event in the fan disk is impossible, the system is failed only if the overall composite fan blades are damaged. For the parallel system, i.e. the first case in Section 3, failure probability for each blade P_{f}^{s} (s=1,⋯,N_{b}) determines the system safety 1-P_{f}. The common two-dimension limit state function, $g_s(\sigma_{\mathrm{e}}, \zeta)=\sigma_{\mathrm{e}}(\sigma_{\mathrm{m}}^{s}(x_1))-\sigma_{\mathrm{a}}^{s}(x_1)$, is formulated, where σ_{a}^{s} denotes the local vibratory stress at a specific sector location, and σ_{e} is material fatigue strength softening by local steady stress σ_{m}^{s}. Therefore, the joint PDF $\pi(\sigma_{\mathrm{e}},\sigma_a)$ is not equal to $\pi(\sigma_{\mathrm{e}})\pi(\sigma_a)$, more complicate than the first two cases. Moreover, using material property listed in Table 5, failure probability in Eq.(22) provide a reference to prediction by ESS based on the direct numerical quadrature (DI).

$$P_{\mathrm{f}}=\prod_{s=1}^{N_{\mathrm{b}}}P_{\mathrm{f}}^{s} \tag{22}$$

Table 5. Composite material fatigue strengths.

σ_{T} /MPa	σ_{C} /MPa	$\sigma_{\mathrm{m}}^{\chi}$ /MPa	$\sigma_{\mathrm{e}}^{\chi}$ /MPa	n_T	n_{C}
2586	1378	275	902	1.7	2.2

The direct quadrature provides a reference value when relative error between two subsequent step is constrained to 1×10^{-12}. For a single composite fan blade, the minimum failure probability is calculated to 1.07×10^{-6} based on numerical integral for each blade failure event. HCF failure probability is 2.69×10^{-26} for fan-disk assembly if these failure events are mutually independent, which determines the upper limit for total failure probability. Amongst blade failure event the smallest probability is selected to validate the effectiveness of ESS. Three samplers employ the corresponding same parameter settings used in Section 2. In Table 6, MCS gives a probability estimate with 8.41% error due to the limited size of sample set. Again, ESS improves prediction provided by SS from -75.89% to -30.19%. Besides, it saves about 6 s in comparison with MCS despite accuracy loss.

To evaluate failure probability of fan-disk assembly, the first two method in Table 6 is implemented foremost. Given high dimensionality, statistical correlations between concentrated ply stresses, it is tough to derive joint PDF to directly calculate failure probability integral. On the other side, MCS obtains a zero failure probability by just drawing 5×10^{7} samples, indicating all samples fall into safe domain and far from enough to ensure CV less than 5%. However, two predictions by subset simulations are feasible, which are listed in Table 7. SS obtains conservative estimation due to an unreasonable acceptance rate. ESS gives the only left failure probability prediction by ten subsets shown in Fig.4. It can be found that the strong correlations between ply stresses distributed in circumferential direction, increases failure probability by a magnitude of ten folds. If HCF failure events for each components in fan-disk assembly are mutually independent, resulting probability is equivalent to an average failure probability 0.306 for each composite fan blade. In this regard, the manufacturers are able to achieve such moderate quality standard, e.g. strictly controlling fabricating defects in composite material.

Table 6. HCF failure probability for a single composite fan blade.

Sampler	P_{f}	Time / s	error	r
DI	1.07×10^{-6}	0.29	1×10^{-12}	1.00
MCS	1.16×10^{-6}	17.88	13.13 (CV / %)	1.00
SS	2.58×10^{-7}	0.24	18.06 (CV / %)	0.87
ESS	7.47×10^{-7}	11.98	41.33 (CV / %)	0.48

Table 7. HCF failure probability for fan-disk assembly.

Sampler	P_{f}	Time / s	CV / %	r
SS	4.67×10^{-11}	0.46	21.74	0.77
ESS	6.86×10^{-10}	17.57	44.35	0.34

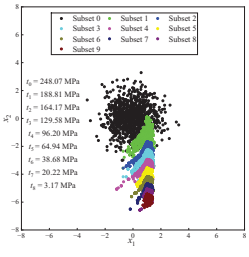

Fig. 4. Samples to evaluate failure probability of mistuned fan-disk assembly by ESS.

5. Conclusion

In this paper ESS is proposed by means of fully exploring random space and adaptively adjusting scale parameter for proposal distribution, which it is found to have a better performance than SS. To obtain samples among a series of subsets, the mixed sampler is to evaluate the intermediate failure probability. Two analytical case demonstrates ESS provides more accurate total failure probability prediction even if computational cost increases by a small extent than SS, but faster than MCS constrained with same size of sample set. They also showcase ESS is not sensitive with how failure domain distributes within random space.

It is integrated into an estimate of HCF failure probability due to harmonic aerodynamic force acting on composite fan blade-disk assembly. For a single blade failure event, ESS again shows great advantage over SS, which reduces prediction error from -75.89% to -30.19%. When MCS and direct quadrature is not feasible for blade-disk assembly even if variability is only from longitudinal elastic modulus for laminas, ESS provides a valuable failure probability prediction considering the statistic correlations in steady and vibratory stresses. This case demonstrates ESS has a promising capacity in engineering reliability analysis, especially for reliability estimation with small size of test data available. In the future, fatigue failure probability of fan disk and associated retention system is to be evaluated. This will enrich engineering application cases to validate ESS.

Acknowledgement

This work was supported by the National Key Research and Development Program of China (No. 2023YFB3709805).

References

[1] Amoo, L.M. (2013). On the design and structural analysis of jet engine fan blade structures. *Progress in Aerospace Sciences*, vol.60, pp.1-11.

[2] Au, S.K. and J.L. Beck (2001). Estimation of small failure probabilities in high dimensions by subset simulation. *Probabilistic Engineering Mechanics*, vol.16, pp. 263-277.

[3] Lan, C.M., Z.Q. Xu, J.M Ma, X.Q. Zhao, and H. Li (2022). Comparison of Markov chain Monte Carlo sampling algorithms in subset sampling, *China Civil Engineering Journal*, vol.55, pp.33-44. (in Chinese)

[4] Goodman, J. and J. Weare (2010). Ensemble sampler with affine invariance. *Communications in Applied Mathematics and Computational Science*, vol.5, pp.65-80.

[5] Lye, A., A. Cicirello, and E. Patelli (2022). An affine and robust sampler for Bayesian inference: transitional ensemble Markov chain Monte carlo. *Mechanical Systems and Signal Processing*, vol.167, p.108471-23.

[6] Reiner, J., N. Linden, R. Vaziri, N. Zobeiry, and B. Krammer (2023). Bayesian parameter estimation for the inclusion of uncertainty in progressive damage simulation of composites. *Composite Structures*, vol.321, p.117257-13.

[7] Xiao, S.N. and W. Nowak (2022). Reliability Sensitivity Analysis Based on a Two-stage Markov Chain Monte Carlo Simulation. *Aerospace Science and Technology*, vol.130, p.107938-11.

[8] Brooks, S.P. and A. Gelman (1998). General methods for monitoring convergence of iterative simulations. *Journal of Computational and Graphical Statistics*, vol.7, pp.434-455.

[9] Tang, X., Y. Chen, and J.G. Zhang (2022). Numerical investigation on HCF weak link locations of a wide-chord laminated composite fan blade with coupled modal vibrations[C]. *Proceedings of ASME Turbo Expo 2022: Turbomachinery Technical Conference and Exposition*, Rotterdam, the Netherlands, June 13-17, GT2022-83613.

[10] Ernst, O., H. Mugler, H.J. Starkloff, and E. Ullmann (2012). On the convergence of generalized polynomial chaos expansions. *ESAIM: Mathematical Modelling. and Numerical Analysis*, vol.46, pp.317-339.

[11] Sandberg, D., R. Mansour, and M. Olsson (2017). Fatigue probability assessment including aleatory and epistemic uncertainty with application to gas turbine compressor blades. *International Journal of Fatigue*, vol.95, pp.132-142.

[12] Liu, X., R.Q. Wang, D.Y. Hu, and J.X. Mao (2020). A calibrated weakest-link model for probabilistic assessment of HCF life considering notch size effects. *International Journal of Fatigue*, vol.137, p.105631-11.